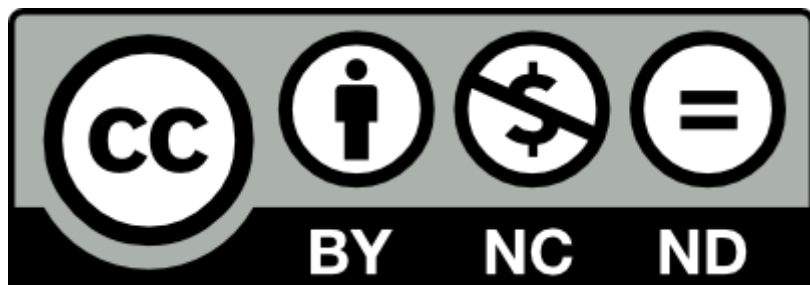


Pedro L. de Hoyos-Martínez, Xabier Erdocia, Fatima Charrier-El Bouhtoury, Raquel Prado, Jalel Labidi, Multistage treatment of almonds waste biomass: characterization and assessment of the potential applications of raw material and products, Waste Management, Volume 80, 2018, Pages 40-50, ISSN 0956-053X <https://doi.org/10.1016/j.wasman.2018.08.051>

(<https://www.sciencedirect.com/science/article/pii/S0956053X18305397>)

Abstract: Almond shells are waste biomass generated in agro-industrial activities, which represent a resource that can be further valorized upon treatment. The purpose of this work was to assess new value-added products obtained through a novel multi-stage delignification process of almond shells. A comprehensive chemical characterization of the raw materials and products involved in each stage of the process was carried out. Moreover, an extensive mass balance was developed, providing a full understanding of the extraction process. The pulps produced did not display a significant cellulose loss and hence they could be exploited as cellulose-rich materials. On the other hand, the obtained lignins presented high purity values ($\approx 90\%$) and a high reactivity, and their structures became more condensed and homogeneous after each extraction cycle. These features would allow their utilization as feedstock of renewable materials such bio-sourced phenolic resins.

Keywords: Almond shells, Waste biomass, Lignin, Cellulose, Renewable products.



Multistage treatment of almonds waste biomass: characterization and assessment of the potential applications of raw material and products

Pedro L. de Hoyos-Martínez^{1,2}, Xabier Erdocia¹, Fatima Charrier-El Bouhtoury², Raquel Prado³, Jalel Labidi^{1*}

¹ *Chemical and environmental engineering department, University of the Basque Country UPV/EHU, Plaza Europa, 1, 20018, San Sebastián, Spain.*

² *CNRS/UNIV PAU & PAYS ADOUR/ E2S UPPA, Institute of Analytical Sciences and Physico-Chemistry for Environment and Materials (IPREM)- IUT des Pays de l'Adour, 371 Rue de Ruisseau, 40004 Mont de Marsan, France.*

³ *Department of Chemistry, Imperial College London, Exhibition Road, SW7 2AZ, London, U.K.*

***Corresponding author:** Jalel Labidi: jalel.labidi@ehu.eus

Abstract: Almond shells are waste biomass generated in agro-industrial activities, which represent a resource that can be further valorized upon treatment. The purpose of this work was to assess new value-added products obtained through a novel multi-stage delignification process of almond shells. A comprehensive chemical characterization of the raw materials and products involved in each stage of the process was carried out. Moreover, an extensive mass balance was developed, providing a full understanding of the extraction process. The pulps produced did not display a significant cellulose loss and hence they could be exploited as cellulose-rich materials. On the other hand, the obtained lignins presented high purity values ($\approx 90\%$) and a high reactivity, and their structures became more condensed and homogeneous after each extraction cycle. These features would allow their utilization as feedstock of renewable materials such bio-sourced phenolic resins.

Keywords: almond shells, waste biomass, lignin, cellulose, renewable products

1. INTRODUCTION

In the current context, the depletion of the fossil fuels claims for a severe shift in the management and utilization of the sources of energy and materials towards a more green and sustainable path. Thus in the last years, there have been a growing tendency in the study and utilization of different types of renewable sources, especially biomass. This growing interest on biomass has been motivated by several factors (Bilgili and Ozturk, 2015): (i) it is an abundant and renewable source, which can be produced anywhere and that represents an option to decrease the dependency to oil; (ii) it provides a solution to poverty in under developed and developing countries, promoting the rural employment and (iii) it contributes to the reduction of the carbon dioxide (CO_2) emissions. Hence, the utilization of biomass as energy source currently is undergoing a great boost worldwide (Ahmad and Tahar, 2014).

Between the different types, the lignocellulosic biomass counts as the most abundant group representing almost 70% of the total plant biomass (Duchesne and Larson, 1989). Lignocellulosic biomass can be originated from diverse sources such as agricultural and forestry residues, municipal wastes (organic and paper) and several crops (Brandt et al., 2013). In this regard, agroforestry activities are said to generate a huge amount of lignocellulosic residues (Zheng et al., 2014). Nevertheless, the overexploitation of forests (especially in developing countries) are jeopardizing this source, which is descending at an alarming rate. Consequently, agricultural wastes are said to be playing a considerable role in the future of forest industry, aiding to the preservation of this natural resource (Guler et al., 2008).

Almonds are an important crop, especially all over the world's temperate regions. Thus, the global world's almond production in 2016 was reported to be around 3.21 million tons distributed in 1.7 million ha (Food and Agriculture Organization of the United Nations Statistics Division (FAOSTAT), 2014). In this sense, Spain is the second world's major producer of almonds (0.2 million tons) after the USA according to FAOSTAT. Almond shells, which are the lignocellulosic material forming the husk of the almond tree fruit, are ranging 35–75% of the total fruit weight (Ebringerová et al., 2007). Hence, between 70 and 150 million kg of this waste are remaining annually in Spain and accordingly, almond shells valorization as a potential source of energy and materials is of great interest. Normally almond shells are burned owing to their higher heating value (HHV) which is comparable to that of forest residues (Chen et al., 2016). Nevertheless, this generates problems such as air pollution, soil erosion and decrease of soil biological activity (Çöpür et al., 2007). Consequently, the valorization of almond shells through their lignocellulosic components (cellulose, hemicellulose and lignin), e.g. for nanopaper manufacturing (Urruzola et al., 2014), bio-oil production (Önal et al., 2014) or as bioadsorbent (Ben Arfi et al., 2017), appears as a more environmentally friendly solution.

On the other hand, lignocellulosic biomass is generally considered as a composite material with a recalcitrant structure composed of three biopolymers namely cellulose, hemicellulose and lignin (Zhao et al., 2012). Lignin which accounts for 10–30 wt% of lignocellulosic biomass (Maity, 2015), is a natural amorphous aromatic complex macromolecule highly crosslinked. It is composed of several subunits i.e. p-hydroxyphenyl (H), guaiacyl (G) and syringyl (S) units,

derived from the coumaryl, coniferyl and sinapyl alcohols respectively (De Wild et al., 2014).

Concerning lignin uses, it is said to be a promising renewable source in several fields due to its aromatic nature (Lora and Glasser, 2002). Accordingly, several potential applications have been reported such as the production of chemicals (Shen et al., 2015), its utilization in materials (Faruk et al., 2016) or its employment as antioxidant (Pouteau et al., 2003). All these potential applications confront with its current situation in the industry, where only the 2% of the lignin industrially produced is used for commercial purposes (Laskar et al., 2013).

Regarding lignin valorization, a key point is the extraction process. Traditionally lignin is produced as a by-product (waste) of the pulp and paper industry. Thus, the most industrially used processes for isolating lignin are sulfate (Kraft) and sulfite (Fernández-Rodríguez et al., 2017). However, they exhibited several disadvantages derived from environmental aspects of the process and the heterogeneity of the lignins. This has triggered a growing interest on the sulfur-free delignification processes such as organosolv, alkaline and ionic liquid pretreatments (Vishtal and Kraslawski, 2011). Organosolv pretreatment is able to isolate high purity lignins, avoiding the significant salt amount formed in alkali process. Thus, the high water consumption required in this pretreatment (Chaturvedi and Verma, 2013) can be avoided reducing the downstream costs. Nevertheless, higher temperatures are needed in organosolv pretreatment compared to the alkali one, which can be performed at ambient temperature (Brodeur et al., 2011).

Regarding the pretreatment with ionic liquids, it allows the fractionation of lignin and hemicellulose without the utilization of volatile organic solvents (as in the

case of organosolv pretreatment). However in organosolv pretreatment, the solvent can be readily recovered by distillation with high yields and low energy consumption, whereas the ionic liquids are difficult to be recycled and reuse (Kumar and Sharma, 2017). Among these sulfur-free extraction methods, organosolv method has drawn considerable attention in the last decades. Organosolv extraction method is an efficient technique for delignification based on the employment of a mixture formed by an organic solvent (mainly alcohols) and water (Wild et al., 2015). The lignin is solubilized into this solvent and the washing liquor and from here, it can be precipitated by lowering the pH.

Several reactions are generally occurring during this pretreatment. The most relevant for lignin extraction, is the hydrolysis of the lignin-hemicellulose linkages and internal lignin bonds via cleavage of the 4-O-methylglucuronic acid ester bonds and α and β -O-aryl ether linkages (Sannigrahi and Ragauskas, 2013). It is known that the cleavage of these aryl ether bonds is responsible for the breakdown of lignin. The α -O-aryl ether are separated more easily, while the β -O-aryl ether linkages need more severe conditions (McDonough, 1993). As mentioned before, through this solubilization lignin and lignin-carbohydrate compounds (in lower extent) can be precipitated from the liquid phase whereas cellulose and some hemicellulose remain in the solid residue.

The high content of cellulose remaining in the solid residue allows its utilization for several applications such as the production of bioethanol. Romaní et al. (2016) studied the use of the solid residue of Eucalyptus wood after organosolv pretreatment for this application. They concluded that process integration of a suitable pretreatment, with intensified SSF stages resulted in a good strategy for

the co-production of high ethanol titers, oligosaccharides and lignin in an integrated biorefinery.

In the organosolv pretreatment, several operational parameters are said to influence the results of the process namely temperature, reaction time, ethanol and catalyst concentration (in case it is needed). Regarding the temperature, it is reported that higher temperatures usually lead to higher percentage of lignin extracted (Kim and Pan, 2010). On the other hand, lignin's solubility in ethanol is maximized at 70% as shown by Ni and Hu 1995 (Ni and Hu, 1995). Concerning the other two parameters, longer times and higher catalyst concentrations provide a bigger extent of delignification (Sannigrahi and Ragauskas, 2013).

In this work, the valorization of almond shells was intended by means of a green extraction process. The extraction of lignin from almond shells was carried out through a novel multi-step organosolv system composed of three sequential extraction stages. Through this system, the maximization of the lignin extraction yields was aimed. Furthermore, the comprehensive characterization of the raw materials and products from each stage and the complete mass balance of the whole extraction process were carried out. Thereby, it was possible to elucidate the selectivity of the process towards the different lignocellulosic compounds, to determine their availability along the whole system and to assess the potential applications of the different products obtained.

2. MATERIALS AND METHODS

2.1 Raw material and equipment

The almond shells, which were provided by local farmers, were coming from almond trees (*Prunus amygdalus*) of the variety *Marcona*. These almond shells were crushed and sieved by means of a Retsch Hammer mill to chips with a size

lower than 1 cm prior to the extraction process. Thus, impurities such as little stones, soil or dust could be removed. The chemical reagents employed for the extraction process and chemical assays were kindly supplied by Sigma-Aldrich.

2.2 Experimental process set up

A multi-step extraction process was developed to maximize the delignification of the almond shells. Thereby three sequential organosolv pulping cycles were carried out resulting in highly pure lignins and rich-cellulose content solid pulps from each cycle. The description of the process set up was provided in Section 1 of supplementary information.

2.2.1 Organosolv process and lignin precipitation

The organosolv delignification process was carried out employing a mixture of ethanol/water (70:30 v/v) at 200 °C during 90 min with a ratio solid to liquid 1:6. During this process, the heat up time was 1.25 h before reaching the set temperature (200 °C). Once the delignification was over, the reactor was cool down during 1 h until the temperature descended to 40–50 °C and the pressure inside the reactor and outside were leveled. These parameters were dependent on the reactor operation.

Regarding the temperature and amount of solvent used for the organosolv process, they were chosen based on a previous work where an optimization was carried out (Toledano et al., 2011). According to this work, the amount of lignin in the liquors is maximized and the amount in the solid residue is minimized, when high temperatures and moderate ethanol concentrations are employed. Nevertheless, temperatures above 200 °C were not desired, since they increase the energy costs and did not show a significant improvement in the amount of

lignin extracted. The process was implemented in a 1.5 L stainless steel Parr Reactor under constant agitation. The liquid phase was separated from the almond shells pulp remaining via filtration. This pulp was washed several times with a mixture of ethanol/water and dried at 50 °C until all the moisture was removed. The liquid phase (black liquor) went through a precipitation step to extract the dissolved lignin. The procedure was done using two volumes of acidified water (pH around 2) per volume of black liquor obtained. The suspension was left to settle overnight to allow a better lignin precipitation. After that, the precipitated lignin in suspension was filtered using polyamide filters (0.22 µm pore size) under vacuum and washed with distilled water until neutral pH was achieved. Finally, the recovered lignin was dried at 50 °C for three days.

2.3 Raw materials characterization

Samples of the raw materials (almond shells and almond shells pulps from the different cycles) were subjected to moisture (TAPPI T264-om-88), ethanol-toluene extractives (TAPPI T204-cm-97) and ashes (TAPPI T244-om-93) quantification. The elucidation of the cellulose, hemicellulose and lignin content was performed by quantitative acid hydrolysis with 72% H₂SO₄ (TAPPI T249-em-85). Prior to this procedure, the raw materials were milled and sieved to particle size lower than 0.25 mm to assure an intimate contact with the reagents utilized and therefore proper characterization results (no over- or underestimations). On the one part, the liquid phase was analyzed via High Performance Liquid Chromatography (HPLC) using a Jasco LC Net II/ADC chromatograph equipped with a refractive index detector and a diode array detector. A sample of the liquid phase was used to quantify the main monosaccharides and degradation products employing a Phenomenex Rezex ROA column; the mobile phase (0.005 N

H_2SO_4) was eluted at a flow rate of 0.35 mL/min at 40 °C. Standards of high purity of D-(+)-glucose, D-(+)-xylose and D-(-)-arabinose were employed as calibration. On the other part, the solid phase obtained from the quantitative acid hydrolysis was oven-dried and its weight was considered as the Klason Lignin. All these procedures were made in triplicate.

2.4 Liquors characterization

The black liquors obtained from the organosolv pulping process were characterized according to different parameters before the lignin precipitation was performed. First pH was determined using a digital CRISON BASIC 20 pH-meter. Density was elucidated by measuring the weight of each liquid fraction in a known volume (10 mL). On the other hand, total dissolved solids (TDS) were calculated using a method based on TAPPI T264 cm-97 to quantify the moisture content in a raw material. Inorganic compounds content (IC) was determined after combustion of the sample in a muffle at 525 °C for 3 h (TAPPI T211 om-93). The organic compounds content (OC) was calculated by the difference between total dissolved (TDS) and inorganic compounds content (IC). Lignin concentration was calculated, as the ratio between the amount of lignin and the volume of black liquor produced.

2.5 Lignin characterization

Once the lignin samples from the different extraction cycles were obtained, they were subjected to several chemical assays to get information about their physicochemical properties, structure and composition.

2.5.1 Chemical characterization of lignin

Several physicochemical parameters of lignin were analyzed to determine the composition and purity of the lignin samples. The Klason lignin (KL) and Acid

soluble lignin (ASL) were elucidated by means of an acidic hydrolysis of the lignin samples in two steps following a procedure carried out by a previous work of this group (Erdocia et al., 2014).

High performance liquid chromatography (HPLC) was used for the determination of the main monosaccharides present in the lignin samples (glucose, xylose and arabinose) and the method was analogous to that described in point 2.3.

Thermogravimetric analysis (TGA) was performed to determine the ash content of the lignin samples using a TGA/STDA RSI analyzer 851 Mettler Toledo. Samples between 4-8 mg were employed and they were subjected to a scanning of temperature 25-1000 °C at a 10 °C/min heating rate in air atmosphere.

2.5.2 High performance size exclusion chromatography (HPSEC)

This analysis was carried out to assess the molecular weight of the lignin samples and their size distribution. The equipment used was a Jasco instrument equipped with an interface LC Net II/ADC, a reflex index detector RI-2031Plus and two PolarGel-M (300mm x 7.5mm) columns displayed in series. The analyses were performed using dimethylformamide with 0.1% lithium bromide as mobile phase and a 0.7 mL/min flow at 40 °C. The equipment was calibrated using polystyrene standards from Sigma-Aldrich ranging between 70000-266 g/mol.

2.5.3 Folin-Ciocalteau assay

This method was carried out to estimate the total hydroxyl groups content of the lignins extracted from the different cycles. In the procedure dimethyl sulphoxide (DMSO>99.5% GC) was used as solvent, gallic acid (>98% HPLC) as standard and samples of lignin 2 g/L in dimethyl sulphoxide (DMSO) were prepared. For the assay, aliquots of 0.5 mL lignin solution were mixed with 2.5 mL of Folin Ciocalteau reagent (Merck) and 5mL Na₂CO₃ and brought to a volume of 50 mL

with distillate water. Following to that, the samples were covered to protect them against light and kept into a thermostatic bath at 40 °C for 30 min. After this time, the absorbance of the samples at 750 nm was measured using a spectrophotometer Jasco V-630 UV with UV quartz cells and a 10 mm light path. The calibration curve was done using solutions of gallic acid in DMSO in the range 100-1000 mg/L. The results were presented as mg of gallic acid equivalents (C_{GAE}) as shown in equation 1.

$$C_{GAE} (\text{mg}_{GAE}/\text{L}) = A / K_{cal} \quad \text{Eq. (1)}$$

Here A makes reference to the absorbance value measured at 750nm and K_{cal} corresponds to the slope of the calibration curve done with gallic acid. These results were presented too as percentage of gallic acid equivalents (%GAE) according to equation 2, where C_{GAE} is the concentration of gallic acid equivalents and C_{sample} is the concentration of the lignin samples.

$$\text{GAE (\%)} = C_{GAE} / C_{sample} \quad \text{Eq. (2)}$$

The results were also calculated as percentage of hydroxyl groups (%OH) as presented in equation 3. Here C_{GAE} is the concentration of gallic acid equivalents, $Mw_{gallic\ acid}$ is the molecular weight of gallic acid, n is the number of hydroxyl groups in gallic acid, Mw_{OH} is the molecular weight of hydroxyl groups and C_{lignin} is the concentration of lignin samples.

$$\text{OH (\%)} = C_{GAE} \cdot (1 / Mw_{gallic\ acid}) \cdot n \cdot Mw_{OH} \cdot (1 / C_{lignin}) \cdot 100 \quad \text{Eq. (3)}$$

2.5.4 Pyrolysis-gas chromatography/Mass spectrometry analysis (Py-GC/MS)

The extracted lignin samples were subjected to pyrolysis-gas chromatography (GC)-mass spectroscopy (MS), to degrade them and break them down to specific lower bonding energy points forming smaller volatile fragments, under inert atmosphere. From these fragments, useful structural information from the lignin

macromolecules can be provided. The analysis and identification of compounds was performed following the procedure described in previous works carried out in the group (Dávila et al., 2017; Fernández-Rodríguez et al., 2017).

2.5.5 2D-Heteronuclear Single Quantum Coherence Spectroscopy (HSQC)-Nuclear Magnetic Resonance (NMR) analysis

The 2D-HSQC-NMR analysis was carried out using a Bruker Avance 600MHz equipment with a z-gradient BBI probe. About 20 mg of lignin sample were dissolved in 6 mL of DMSO (DMSO-d6) prior to the analysis. The spectral widths were 5000 and 25 000 Hz for the ¹H and ¹³C dimensions, respectively.

2.5.6 Thermogravimetric analysis (TGA)

Thermogravimetric analysis was carried out in a TGA/STDA RSI analyzer 851 Mettler Toledo. In order to assess the thermal degradation behavior of the lignin, 4-8 mg of each lignin sample were tested under inert atmosphere (50 mL/min of N₂) between 25-800 °C at a heating rate of 10 °C/min.

3. RESULTS AND DISCUSSION

3.1 Raw material and process characterization

3.1.1 Chemical composition of raw materials

The characterization of the raw materials used in the subsequent extraction stages was performed to know their initial composition. The results are enclosed in table 1 and presented in terms of percentages of cellulose, hemicelluloses, lignin, extractive and ashes.

Regarding the almond shells, the composition was in accordance with the values of other works from the literature (Nabarlatz et al., 2007; Sequeiros et al., 2014). Nevertheless, slight differences were observed owing to the characterization technique employed or the grain size of the material prior to characterization. In

this study quantitative acid hydrolysis (TAPPI T249-em-85) was performed instead of other TAPPI norms used generally for wood characterization. Besides, the almond shells were milled and sieved to a size small enough to assure the intimate contact between the reagents and the raw material (0.5 mm). Therefore, some tiny differences were observed (especially in the lignin content) comparing to the literature.

Regarding the content of the different components, hemicellulose and lignin were said to be majorly present. The high lignin content proved the potential and suitability of this raw material in lignin valorization for latter applications.

Concerning the almond shell pulps (ASP), the content of the different components varied substantially from that of the raw material. Indeed the content of the two main components (hemicelluloses and lignin) was considerably reduced. In the case of hemicellulose such a decrease was caused by the harsh conditions of pressure and temperature employed, which led to its degradation. On the other side, the lignin reduction was expected since it was the goal of the organosolv treatment. Respecting the content of cellulose and extractives, an increasing tendency was observed. Nonetheless, the content of the former underwent a substantial boost whereas the percentage of the latter grew slightly. These rises did not imply though that the amounts of cellulose and extractives were bigger in the ASPs than in AS but that they diminished less than hemicellulose and lignin contents. This will be shown and confirmed in the mass balance afterwards.

When comparing the content of the different components in the ASPs, two clear tendencies could be regarded. On the one hand, the content of cellulose was increasing, mainly from the ASP1 to the ASP2. On the other hand, the content of

the rest of the components tended to decrease. The amount of ashes in the ASPs was said to be negligible considering that it was too low to be detected.

3.1.2 Efficiency of the process extraction cycles

The effectiveness of the different cycles was assessed in terms of lignin extraction yields (overall, relative, total amount extracted yield) and yields of ASPs (Table 2).

From the previous results it can be observed that high extraction yields were obtained for the first cycle, whereas lower efficiencies were achieved for the second and third. The reason for that was that after each extraction cycle the amount of lignin available was lower and therefore less lignin could be extracted. On the contrary, the yields of ASP were increasing as the cycles passed by, owing to the reduction of the pulp solubility. These two tendencies were interrelated and hence, the fact that in each cycle less amount of pulp was dissolved, resulted in less amount of lignin transferred from the pulp to the liquor and therefore less amount of lignin recovered. After the three consecutive extraction cycles, 87.73% of the total lignin present in the almond shells at the beginning was recovered. This yield was comparable to that obtained in a precedent work (89.40%) (Fernández-Rodríguez et al., 2017).

3.1.3 Process mass balance

Once the chemical characterization of the raw material and pulps was known and their yields elucidated, a mass balance of the whole system was carried out. Thereby, the variations in the amounts of different components through the cycles could be monitored. The balance was based on the quantity of almond shells fed into the reactor at the beginning of cycle 1 (100 g). The results of the mass balance are presented in Table 3. In regards to these data, it was proved that

after the first cycle the majority of the lignin was extracted. Similar to lignin, more than the half of the hemicellulose amount was degraded in this stage. On the other hand, the amount of cellulose amount remained almost intact between AS and ASP1. Taking these previous tendencies into consideration, it can be explained the great increase of cellulose percentage displayed in Table 1. The reason for that was that the amounts of hemicellulose and lignin decreased highly after first extraction cycle and hence cellulose became the major component in the pulps.

Concerning the second extraction cycle, it appeared to be not so effective to the lignin as the first one was. Thereby, no big differences were encountered in the composition between ASP1 and ASP2. The bigger reduction was regarded in the hemicellulose content, although again it was much lower than that of the first cycle. This was a result of the pulp degradation, owing to the high temperature and pressure underwent during the extraction. The amount of the rest of the components slightly decreased, as a consequence of these conditions. Third cycle showed only a small reduction in the extraction efficiency for all the components. The reason for this loss of efficiency compared to the other cycles was that the pulp was already too degraded and saturated from the previous extraction processes at such severe conditions.

Regarding the total extraction of the different components, lignin (which was recovered) and hemicellulose were majorly extracted by the end of the third stage. On the other hand, the amount of cellulose did not go through a significant change, since almost 70% of the initial content remained after the whole extraction process.

3.2 Liquor characterization

The main physicochemical parameters of the liquid fraction obtained from the delignification processes were assessed and summarized in Table 4.

The values of the pH and density were similar for all the liquor samples since the conditions used for the almond shells delignification were the same. Regarding the TDS, LC and OC, a reduction was observed from the liquor C1 to the liquor C3. It must be noted that the TDS content was almost completely associated to the OC content, since no inorganic matter was detected in the liquors. Focusing on the OC and LC contents it was concluded that both parameters were highly related since it was expected that the lignin in the liquor accounted for the majority of the organic compounds. For this reason, both parameters were reduced after the sequential extractions. The main reduction was observed between the first and the second extraction cycle (from 35.17 to 8.34 g·L⁻¹). This was in agreement and also helped explaining the reduction of the lignins extraction yields mentioned in the previous section (especially between the two first delignification steps). Thus, as the lignin content in the liquor, was dramatically diminished there was a lower amount of lignin available to be extracted resulting in a much lower yield.

3.3 Lignin characterization

3.3.1 Lignin chemical composition

The characterization of all the lignins samples was determined for elucidating their chemical composition (Table 5).

The different lignin samples showed high KL percentage and therefore high purity ($\approx 90\%$), as was expected for organosolv lignins (Huijgen et al., 2014). The values were similar and within a narrow range, since they were extracted from the same feedstock under analogous circumstances. This implies that sequential extraction

process did not jeopardize the purity of the lignins extracted. Respecting acid soluble lignin content, the values tended to slowly decrease from extraction stage to extraction stage due to the delignification processes.

On the other side, lignin was also said to yield lignin carbohydrate complexes (LCC) owing to non-covalent interactions and oxidative reactions with polysaccharides (You et al., 2015). These compounds represented certain percentage in the lignin content, considered impurities, which was assessed by measuring the sugar content. The sugar content in the lignin samples was low proving once more their high purity. This content was increasing following the delignification processes. The reason for that was assumed to be that the lignins from the different steps were gradually becoming more condensed and with stronger linkages. Thus, the removal of the remaining sugars impurities was hindered as the stages went by. Xylose was the main sugar from the hemicellulose fraction found in the lignins. This was in agreement with that reported by Gordobil et al. 2014 (Gordobil et al., 2014). This trend was not observed in the lignin from the last extraction cycle, which had a higher amount of glucose. In this case, the bigger presence of glucose could indicate that at the last stage some cellulose was removed from the ASP. The harsh conditions underwent by the pulp sample after 3 cycles, would have caused the dissolution of cellulose along with the lignin.

3.3.2 High performance size exclusion chromatography (HPSEC)

This chromatographic technique was performed in order to determine the lignins size and its distribution. The main parameters measured were the weight average (M_w), number average molecular weights (M_n) and polydispersity index (M_w/M_n).

Marked tendencies can be regarded from the previous results. In respect to weight average and number average molecular weights, they did not present considerable divergences, between 6371-6730 g/mol and 1286-1775 g/mol respectively. The values were low and within the typical range of organosolv lignins (Wild et al., 2015). Nevertheless, they increased following the successive lignin extraction steps. This tendency pointed out that at the beginning the lignin structure was more branched, the linkages were broken more easily and therefore the remaining fragments had lower molecular weight. However, as the delignification stages moved forward, the lignin structure became more condensed and the linkages were more difficult to break leading to a slightly higher molecular weight lignin.

Regarding polydispersity index, the tendency was the opposite to that of the molecular weights, between 4.96-3.79. Thus, it was proved that the lignins obtained in the final stages (more difficult to be extracted) had a more condensed structure owing to the increase of the C-C bonds and were more stable.

3.3.3 Total Hydroxyl content (Folin-Ciocalteau Assay)

The quantification of the relative content of hydroxyl groups in the different lignin samples was done using the Folin Ciocalteau assay. This is really important, since the content of hydroxyl groups is said to be a good indicator of the lignin's reactivity (Goldmann et al., 2016) and provides a point of comparison between different lignins concerning their potential applications. The results were calculated in terms of concentration of gallic acid equivalents (C_{GAE}), percentage of gallic acid equivalents (%GAE) and percentage of hydroxyl groups (%OH) and were presented in Fig. 1.

The values obtained for the previous parameters were comparable to those reported in other works in the literature for organosolv lignins (dos Santos et al., 2014; Erdocia et al., 2014). Besides, it was observed that these parameters were decreasing following the sequential delignification steps. This fact would indicate a degradation of the phenolic compounds owing to the extraction steps at harsh conditions (García et al., 2012). Moreover, these severe treatments were said to promote the solution of more components from the raw material (García et al., 2010). Thus, the lignin samples could have a higher amount of impurities and therefore present lower hydroxyl groups concentrations. This was confirmed in the present work according to the previous chemical characterization of lignins where the amount of sugars contained in the samples was increasing after each delignification stage.

The reduction of hydroxyl groups proved as well that the lignins extracted after the consecutive cycles presented a more condensed structure.

On the contrary, the higher content of hydroxyl groups in the lignin extracted in the first cycle compared to the others highlighted its higher reactivity.

3.3.4 Analysis of lignin composition by Py-GC/MS

The pyrolysis analysis yielded a huge and heterogeneous number of compounds (phenols, acids, esters and ketones), from which the phenolic ones were found to be the most abundant group. Phenols are related to the lignins reactivity and they can play an important role in potential applications. For this reason, special focus was put over this group and they were properly assessed. The mentioned phenols were classified into different subcategories, depending on the substituents as reported by Chen et al. 2015 (Chen et al., 2015). Thereby five

groups of compounds namely benzene type (B), phenol type (P), catechol type (C), guaiacol type (G) and syringol type (S) were defined.

It was known that the relative content of each component varied with the pyrolytic temperature (Ma et al., 2016). Hence, a scanning of temperatures was carried out for the sample L1 to evaluate the distribution of products derived from the pyrolysis at each case (Section 3 of supplementary information).

Following the scanning of temperatures, the optimal value was selected at 600°C. Thereby the lignin samples L2 and L3 were subjected to pyrolysis at this temperature. Then, the assessment of the products from the pyrolysis of the different lignin samples was performed. The identification and characterization of the main phenolic compounds and derivatives produced during the pyrolysis is included in Table 6.

From the previous results it was seen that the amount of phenolic compounds identified and quantified in the L1 and L2 was similar (small reduction from 57,18% L1 to 53,29% L2). Nevertheless, the relative content of phenolic units identified in the L3 was much lower compared to the previous ones (decrease from 53,29% L2 to 33,37% L3). Regarding the different phenolic groups it could be remarked that no considerable amount of benzene derivatives was found in the different lignin samples. Phenol and catechol derivatives presented comparable contents and tendencies. Concerning guaiacyl and syringyl derivatives, there was a global reduction following the consecutive delignification steps. Besides the content of syringyl type compounds was higher than the guaiacyl one in all the lignin samples, yielding S/G ratios higher to one. Taking these results into consideration, it was concluded that despite being a non woody lignin source, almond shells could be considered as a hard wood, since the

selectivity to syringyl type units was higher than that of guaiacyl ones (Asmadi et al., 2011; Constant et al., 2016). On the other side, the highest S/G ratio was obtained for the L1, whereas the L2 and L3 ones were lower and similar. This was in accordance with the work by Lourenço et al., (2012) who reported that the syringyl-rich lignins were more easily cleaved and solubilised. Moreover, since high S/G ratios were known to induce high lignin reactivity (Chiang, 2005), L1 was said to be the more reactive. In addition to that, the fact that the L2 and L3 showed lower S/G ratios than L1, confirmed the more condensed structure of those lignins as reported by Sun et al. 2016 (Sun et al., 2016). Moreover, when comparing L2 and L3 samples the latter was said to have a more condensed structure because the selectivity to phenolic derivatives after pyrolysis presented a strong reduction.

3.3.5 Analysis of lignin composition by HSQC-RMN

The heteronuclear single quantum coherence (HSQC) NMR analysis was performed to complement and evaluate the information elucidated by Py-GC/MS analysis. The spectra from the different lignin samples were depicted in Fig. 2. They include correlations in two differentiated regions: aliphatic (δ_C/δ_H 50-95/2.5-6 ppm) and aromatic (δ_C/δ_H 95-160/5.5-8 ppm).

It is known that this technique represents a powerful tool for the characterization of the lignin structure, giving information on the interunit linkages present and the lignin aromatic units (Prado et al., 2016). Thus, the main assigned structures from the spectra were presented in Fig. 3. The different structures in lignin samples and the cross signals were assigned based on previous studies performed by several authors (Rencoret et al., 2009; Wen et al., 2013; Yuan et al., 2011).

Lignin side-chain region. This region of the spectra ($\delta_{\text{C}}/\delta_{\text{H}}$ 50-95/2.5-6 ppm) provided structural information, especially about the interunit linkages present in lignin. Thereby, the three typical bonds in lignin namely β -O-4' (A, A'), β - β (B) and β -5' (C), could be observed in the spectra. Other prominent signals were seen corresponding to methoxyl groups ($\delta_{\text{C}}/\delta_{\text{H}}$ 56.30/3.75). In addition to that, associated carbohydrates were found as well in this region. Thus benzylether lignin carbohydrate complexes (LCC) were encountered at ($\delta_{\text{C}}/\delta_{\text{H}}$ 81.00/4.51).

Aromatic region. In this region ($\delta_{\text{C}}/\delta_{\text{H}}$ 95-160/5.5-8 ppm) the major signals were associated mainly to syringyl (S) and guaiacyl (G) units. The S units displayed the most prominent signal, especially for the correlation C_{2,6}-H_{2,6} at $\delta_{\text{C}}/\delta_{\text{H}}$ 104.27/6.65. Other signals regarded in the aromatic region were those associated to cinnamaldehyde end groups (I).

Regarding the relative quantification of the lignin interunits in the HSQC spectra, two methods are commonly used (Constant et al., 2016). On the one hand, the utilization of the aromatic units as internal standard, which takes the signal of syringyl and guaiacyl peaks. On the other side, the use of the signal intensity from the entire region. Afterwards the results are presented either as percentage of 100 aromatic units or either as percentage of total side chains. For the first method several equations are reported depending on the type of lignin assessed (softwood, hardwood, grass lignins) (Wen et al., 2013). In our case, the problem was that the lignin did not strictly belong to any of the categories and therefore the second method was selected. The results of the interunit relative abundance are presented in Table 7.

From the previous results, it was seen that the amount of methoxyl groups was decreasing through the different cycles and therefore lignins were becoming less

branched. Hence, it was confirmed the fact that after each extraction cycle the lignins present a more condensed structure. On the other hand, only small percentages of lignin LCC (impurities) were found proving once more the high purity of the lignins. Moreover, this group presented an increasing tendency from the first to the third extraction cycle. This was also in accordance with the results presented in Section 3.3.1 where the chemical analysis of the lignins was done. Concerning the S/G ratios, the values displayed the same tendency obtained in the Py-GC/MS analysis. Thus, the conclusions presented in the previous Section 3.3.4 were corroborated.

3.3.6 Thermogravimetric analysis (TGA/DTGA)

The thermal stability of the different lignins and their decomposition was studied and thus the thermogravimetric (TG) and the first derivative thermogravimetric (DTG) curves were determined and presented in Fig. 4A and B. From these figures, important parameters such as the weight loss of the lignins related to the temperature and their weight loss rate could be extracted.

Fig. 4A showed that the lignins degradation took place throughout a broad range of temperatures, due to the complexity of the lignins structure (Schorr et al., 2014). This was also explained by the fact that lignins presented several functional groups containing oxygen, which have different thermal stabilities (Brebu and Vasile, 2010). Consequently, several weight loss stages could be seen for all the lignin samples. The first weight loss was due to the moisture evaporation of the lignins below 100 °C (Gordobil et al., 2016). Then, a second stage was regarded within a range between 325-375 °C related to the cleavage of ether inter-units linkage (Bertini et al., 2012), which constituted the main degradation step. Following that, the split of the aliphatic side chains and other

structural units occurs as well (Laurichesse and Avérous, 2014). Finally, at 800 °C a char residue still remained because of the rearrangement of lignin structure at high temperatures.

The thermal stability of the samples was evaluated by several parameters presented in Table 8, namely initial degradation temperature ($T_{5\%}$), maximum degradation temperature (T_{max}) and char residue remaining at the final temperature.

It can be seen from these results that the L1 and L2 presented similar behaviour concerning the initial and the maximum degradation temperatures and higher than L3. However, all these temperatures were within a narrow range, showing that all the different lignins presented a similar thermal behaviour. Regarding the char residue remaining, the percentages of L2 and L3 were similar and higher compared to the L1. Fig. 4B showed that lignins decomposition presented a wide peak due to their polydispersity. Indeed, it was noted that the wideness of the peak was decreasing as lignin sequential extraction moved forward. This was in agreement with their polydispersity, which was also decreasing from L1 to L3.

3.4 Products applications

Regarding the lignin produced, a high purity and reactivity were observed according to the results presented before. These features would allow its use of for several potential applications. For instance, the employment of lignin as component of phenolic resins depending on its low molecular weights and reactivity has been already reported (Zhang et al., 2013). In this worl, it was already confirmed a significant content of hydroxyl groups in the lignins leading to a high reactivity. Additionally the lignins molecular presented low molecular weights. Hence, they could be utilize in the synthesis of phenolic resins to replace

other phenolic components of non-renewable nature. The use of lignins as reinforcement in composites has been lately reported (Dias et al., 2016). In this sense, according the lignin features presented in this work it would be a potential application as well. In other work the lignin majorly and cellulose in a minor extent, were observed to significantly enhance the decoloration efficiency of medical wastes for solid fuel production (Shen et al., 2017). Since lignin and cellulose were the main components produced in this process, this would represent another potential application.

Concerning the cellulose-rich pulps obtained during the process, the main application could be the production of bioethanol by enzymatic hydrolysis and further fermentation or the use for materials applications by the production of nanofibrils (Deepa et al., 2015).

4. CONCLUSIONS

In this work the valorization of almonds shells, as waste biomass generated from the agriculture, was achieved by means of a multi-step organosolv process. On the one hand, the pulps remaining after each extraction stage showed a very slight increment in the cellulose content. However, as it was the major component, they could be utilized as cellulose-rich material for further applications. On the other hand, a high lignin recovery at the end of the extraction process was accomplished (87.73%), with high purity values ($\approx 90\%$), high reactivity (high hydroxyl group content and S/G ratios) and low molecular weights. These features were of great interest, since they would allow the lignin utilization as feedstock for renewable materials such as biosourced phenolic resins or as reinforcement for biocomposites.

5. ACKNOWLEDGEMENTS

The authors thank the University of the Basque Country UPV/EHU, and the University of Pau and Pays de l'Adour UPPA (Predoctoral fellowship-PIFPAU 15/01) and Spanish Ministry of Science, Innovation and Universities (CTQ2016-78689-R) for financially supporting this work.

References

- Ahmad, S., Tahar, R.M., 2014. Selection of renewable energy sources for sustainable development of electricity generation system using analytic hierarchy process: A case of Malaysia. *Renew. Energy* 63, 458–466.
<https://doi.org/10.1016/J.RENENE.2013.10.001>
- Asmadi, M., Kawamoto, H., Saka, S., 2011. Thermal reactions of guaiacol and syringol as lignin model aromatic nuclei. *J. Anal. Appl. Pyrolysis* 92, 88–98.
<https://doi.org/10.1016/J.JAAP.2011.04.011>
- Ben Arfi, R., Karoui, S., Mougin, K., Ghorbal, A., 2017. Adsorptive removal of cationic and anionic dyes from aqueous solution by utilizing almond shell as bioadsorbent. *Euro-Mediterranean J. Environ. Integr.* 2, 20. <https://doi.org/10.1007/s41207-017-0032-y>
- Bertini, F., Canetti, M., Cacciamani, A., Elegir, G., Orlandi, M., Zoia, L., 2012. Effect of ligno-derivatives on thermal properties and degradation behavior of poly(3-hydroxybutyrate)-based biocomposites. *Polym. Degrad. Stab.* 97, 1979–1987.
<https://doi.org/10.1016/J.POLYMDEGRADSTAB.2012.03.009>
- Bilgili, F., Ozturk, I., 2015. Biomass energy and economic growth nexus in G7 countries: Evidence from dynamic panel data. *Renew. Sustain. Energy Rev.* 49, 132–138. <https://doi.org/10.1016/J.RSER.2015.04.098>
- Brandt, A., Gräsvik, J., Hallett, J.P., Welton, T., 2013. Deconstruction of lignocellulosic biomass with ionic liquids. *Green Chem.* 15, 550.
<https://doi.org/10.1039/c2gc36364j>
- Brebu, M., Vasile, C., 2010. Thermal degradation of lignin—a review. *Cellul. Chem. Technol.* 44, 353.
- Brodeur, G., Yau, E., Badal, K., Collier, J., Ramachandran, K.B., Ramakrishnan, S., 2011. Chemical and physicochemical pretreatment of lignocellulosic biomass: a review. *Enzyme Res.* 2011, 787532. <https://doi.org/10.4061/2011/787532>
- Chaturvedi, V., Verma, P., 2013. An overview of key pretreatment processes employed for bioconversion of lignocellulosic biomass into biofuels and value added products. *3 Biotech* 3, 415–431. <https://doi.org/10.1007/s13205-013-0167-8>
- Chen, K., Escott, C., Loira, I., del Fresno, J., Morata, A., Tesfaye, W., Calderon, F., Benito, S., Suárez-Lepe, J., 2016. The Effects of Pre-Fermentative Addition of Oenological Tannins on Wine Components and Sensorial Qualities of Red Wine.

Molecules 21, 1445. <https://doi.org/10.3390/molecules21111445>

Chen, L., Wang, X., Yang, H., Lu, Q., Li, D., Yang, Q., Chen, H., 2015. Study on pyrolysis behaviors of non-woody lignins with TG-FTIR and Py-GC/MS. *J. Anal. Appl. Pyrolysis* 113, 499–507. <https://doi.org/10.1016/J.JAAP.2015.03.018>

Chiang, V.L., 2005. Understanding gene function and control in lignin formation in wood. *Agric. Biotechnol.* 17, 139–144.

Constant, S., Wienk, H.L.J., Frissen, A.E., Peinder, P. de, Boelens, R., van Es, D.S., Grisel, R.J.H., Weckhuysen, B.M., Huijgen, W.J.J., Gosselink, R.J.A., Bruijnincx, P.C.A., 2016. New insights into the structure and composition of technical lignins: a comparative characterisation study. *Green Chem.* 18, 2651–2665.
<https://doi.org/10.1039/C5GC03043A>

Çöpür, Y., Güler, C., Akgül, M., Taşçıoğlu, C., 2007. Some chemical properties of hazelnut husk and its suitability for particleboard production. *Build. Environ.* 42, 2568–2572. <https://doi.org/10.1016/J.BUILDENV.2006.07.011>

Dávila, I., Gullón, P., Andrés, M.A., Labidi, J., 2017. Coproduction of lignin and glucose from vine shoots by eco-friendly strategies: Toward the development of an integrated biorefinery. *Bioresour. Technol.* 244, 328–337.
<https://doi.org/10.1016/J.BIORTECH.2017.07.104>

De Wild, P.J., Huijgen, W.J.J., Gosselink, R.J.A., 2014. Lignin pyrolysis for profitable lignocellulosic biorefineries. *Biofuels, Bioprod. Biorefining* 8, 645–657.
<https://doi.org/10.1002/bbb.1474>

Deepa, B., Abraham, E., Cordeiro, N., Mozetic, M., Mathew, A.P., Oksman, K., Faria, M., Thomas, S., Pothan, L.A., 2015. Utilization of various lignocellulosic biomass for the production of nanocellulose: a comparative study. *Cellulose* 22, 1075–1090.
<https://doi.org/10.1007/s10570-015-0554-x>

Dias, O.A.T., Negrão, D.R., Silva, R.C., Funari, C.S., Cesarino, I., Leao, A.L., 2016. Studies of lignin as reinforcement for plastics composites. *Mol. Cryst. Liq. Cryst.* 628, 72–78. <https://doi.org/10.1080/15421406.2015.1137677>

dos Santos, P.S.B., de Cademartori, P.H.G., Prado, R., Gatto, D.A., Labidi, J., 2014. Composition and structure of organosolv lignins from four eucalypt species. *Wood Sci. Technol.* 48, 873–885. <https://doi.org/10.1007/s00226-014-0646-z>

Duchesne, L.C., Larson, D.W., 1989. Cellulose and the Evolution of Plant Life. *Bioscience* 39, 238–241. <https://doi.org/10.2307/1311160>

- Ebringerová, A., Hromádková, Z., Košťálová, Z., Sasinková, V., 2007. CHEMICAL VALORIZATION OF AGRICULTURAL BY-PRODUCTS: ISOLATION AND CHARACTERIZATION OF XYLAN-BASED ANTIOXIDANTS FROM ALMOND SHELL BIOMASS. *BioResources* 3, 60–70. <https://doi.org/10.15376/biores.3.1.60-70>
- Erdocia, X., Prado, R., Corcuera, M.Á., Labidi, J., 2014. Influence of Reaction Conditions on Lignin Hydrothermal Treatment. *Front. Energy Res.* 2, 13. <https://doi.org/10.3389/fenrg.2014.00013>
- Faruk, O., Obaid, N., Tjong, J., Sain, M., Tjong, J., Sain, M., 2016. Lignin Reinforcement in Thermoplastic Composites, in: Lignin in Polymer Composites. Elsevier, pp. 95–118. <https://doi.org/10.1016/B978-0-323-35565-0.00006-0>
- Fernández-Rodríguez, J., Gordobil, O., Robles, E., González-Alriols, M., Labidi, J., 2017. Lignin valorization from side-streams produced during agricultural waste pulping and total chlorine free bleaching. *J. Clean. Prod.* 142, 2609–2617. <https://doi.org/10.1016/J.JCLEPRO.2016.10.198>
- Food and Agriculture Organization of the United Nations Statistics Division (FAOSTAT), 2014. Production/Crops for almonds with shell (database).
- García, A., González Alriols, M., Spigno, G., Labidi, J., 2012. Lignin as natural radical scavenger. Effect of the obtaining and purification processes on the antioxidant behaviour of lignin. *Biochem. Eng. J.* 67, 173–185. <https://doi.org/10.1016/J.BEJ.2012.06.013>
- García, A., Toledano, A., Andrés, M.Á., Labidi, J., 2010. Study of the antioxidant capacity of Miscanthus sinensis lignins. *Process Biochem.* 45, 935–940. <https://doi.org/10.1016/J.PROCBIO.2010.02.015>
- Goldmann, W.M., Ahola, J., Mankinen, O., Kantola, A.M., Komulainen, S., Telkki, V.-V., Tanskanen, J., 2016. Determination of Phenolic Hydroxyl Groups in Technical Lignins by Ionization Difference Ultraviolet Spectrophotometry ($\Delta\epsilon$ -IDUS method). *Period. Polytech. Chem. Eng.* 61, 93–101. <https://doi.org/10.3311/PPch.9269>
- Gordobil, O., Egüés, I., Llano-Ponte, R., Labidi, J., 2014. Physicochemical properties of PLA lignin blends. *Polym. Degrad. Stab.* 108, 330–338. <https://doi.org/10.1016/J.POLYMDEGRADSTAB.2014.01.002>
- Gordobil, O., Moriana, R., Zhang, L., Labidi, J., Sevastyanova, O., 2016. Assesment of technical lignins for uses in biofuels and biomaterials: Structure-related properties, proximate analysis and chemical modification. *Ind. Crops Prod.* 83, 155–165.

<https://doi.org/10.1016/J.INDCROP.2015.12.048>

Guler, C., Copur, Y., Tascioglu, C., 2008. The manufacture of particleboards using mixture of peanut hull (*Arachis hypoaea L.*) and European Black pine (*Pinus nigra Arnold*) wood chips. *Bioresour. Technol.* 99, 2893–2897.

<https://doi.org/10.1016/J.BIORTECH.2007.06.013>

Huijgen, W.J.J., Telysheva, G., Arshanitsa, A., Gosselink, R.J.A., de Wild, P.J., 2014. Characteristics of wheat straw lignins from ethanol-based organosolv treatment. *Ind. Crops Prod.* 59, 85–95. <https://doi.org/10.1016/J.INDCROP.2014.05.003>

Kim, D.-E., Pan, X., 2010. Preliminary Study on Converting Hybrid Poplar to High-Value Chemicals and Lignin Using Organosolv Ethanol Process. *Ind. Eng. Chem. Res.* 49, 12156–12163. <https://doi.org/10.1021/ie101671r>

Kumar, A.K., Sharma, S., 2017. Recent updates on different methods of pretreatment of lignocellulosic feedstocks: a review. *Bioresour. Bioprocess.* 4, 7. <https://doi.org/10.1186/s40643-017-0137-9>

Laskar, D.D., Yang, B., Wang, H., Lee, J., 2013. Pathways for biomass-derived lignin to hydrocarbon fuels. *Biofuels, Bioprod. Biorefining* 7, 602–626. <https://doi.org/10.1002/bbb.1422>

Laurichesse, S., Avérous, L., 2014. Chemical modification of lignins: Towards biobased polymers. *Prog. Polym. Sci.* 39, 1266–1290. <https://doi.org/10.1016/J.PROGPOLYMSCI.2013.11.004>

Lora, J.H., Glasser, W.G., 2002. Recent Industrial Applications of Lignin: A Sustainable Alternative to Nonrenewable Materials. *J. Polym. Environ.* 10, 39–48. <https://doi.org/10.1023/A:1021070006895>

Lourenço, A., Gominho, J., Marques, A.V., Pereira, H., 2012. Reactivity of syringyl and guaiacyl lignin units and delignification kinetics in the kraft pulping of *Eucalyptus globulus* wood using Py-GC–MS/FID. *Bioresour. Technol.* 123, 296–302. <https://doi.org/10.1016/J.BIORTECH.2012.07.092>

Ma, Z., Sun, Q., Ye, J., Yao, Q., Zhao, C., 2016. Study on the thermal degradation behaviors and kinetics of alkali lignin for production of phenolic-rich bio-oil using TGA–FTIR and Py–GC/MS. *J. Anal. Appl. Pyrolysis* 117, 116–124. <https://doi.org/10.1016/J.JAAP.2015.12.007>

Maity, S.K., 2015. Opportunities, recent trends and challenges of integrated biorefinery: Part I. *Renew. Sustain. Energy Rev.* 43, 1427–1445. <https://doi.org/10.1016/J.RSER.2014.11.092>

- McDonough, T., 1993. The chemistry of organosolv delignification. *TAPPI J.* 76, 186–193.
- Nabarlatz, D., Ebringerová, A., Montané, D., 2007. Autohydrolysis of agricultural by-products for the production of xylo-oligosaccharides. *Carbohydr. Polym.* 69, 20–28. <https://doi.org/10.1016/J.CARBPOL.2006.08.020>
- Ni, Y., Hu, Q., 1995. Alcell® lignin solubility in ethanol–water mixtures. *J. Appl. Polym. Sci.* 57, 1441–1446. <https://doi.org/10.1002/app.1995.070571203>
- Önal, E., Uzun, B.B., Pütün, A.E., 2014. Bio-oil production via co-pyrolysis of almond shell as biomass and high density polyethylene. *Energy Convers. Manag.* 78, 704–710. <https://doi.org/10.1016/J.ENCONMAN.2013.11.022>
- Pouteau, C., Dole, P., Cathala, B., Averous, L., Boquillon, N., 2003. Antioxidant properties of lignin in polypropylene. *Polym. Degrad. Stab.* 81, 9–18. [https://doi.org/10.1016/S0141-3910\(03\)00057-0](https://doi.org/10.1016/S0141-3910(03)00057-0)
- Prado, R., Erdocia, X., De Gregorio, G.F., Labidi, J., Welton, T., 2016. Willow Lignin Oxidation and Depolymerization under Low Cost Ionic Liquid. *ACS Sustain. Chem. Eng.* 4, 5277–5288. <https://doi.org/10.1021/acssuschemeng.6b00642>
- Rencoret, J., Marques, G., Gutiérrez, A., Nieto, L., Jiménez-Barbero, J., Martínez, Á.T., del Río, J.C., 2009. Isolation and structural characterization of the milled-wood lignin from Paulownia fortunei wood. *Ind. Crops Prod.* 30, 137–143. <https://doi.org/10.1016/J.INDCROP.2009.03.004>
- Romaní, A., Ruiz, H.A., Teixeira, J.A., Domingues, L., 2016. Valorization of Eucalyptus wood by glycerol-organosolv pretreatment within the biorefinery concept: an integrated and intensified approach. *Renew. Energy* 95, 1–9, <https://doi.org/10.1016/J.RENENE.2016.03.106>
- Sannigrahi, P., Ragauskas, A.J., 2013. Fundamentals of Biomass Pretreatment by Fractionation, in: Aqueous Pretreatment of Plant Biomass for Biological and Chemical Conversion to Fuels and Chemicals. John Wiley & Sons, Ltd, Chichester, UK, pp. 201–222. <https://doi.org/10.1002/9780470975831.ch10>
- Schorr, D., Diouf, P.N., Stevanovic, T., 2014. Evaluation of industrial lignins for biocomposites production. *Ind. Crops Prod.* 52, 65–73. <https://doi.org/10.1016/J.INDCROP.2013.10.014>
- Sequeiros, A., Gatto, D.A., Labidi, J., Serrano, L., 2014. Different extraction methods to obtain lignin from almond shell. *J. Biobased Mater. Bioenergy* 8, 370–376.

- Shen, D., Liu, G., Zhao, J., Xue, J., Guan, S., Xiao, R., 2015. Thermo-chemical conversion of lignin to aromatic compounds: Effect of lignin source and reaction temperature. *J. Anal. Appl. Pyrolysis* 112, 56–65.
<https://doi.org/10.1016/J.JAAP.2015.02.022>
- Shen, Y., Yu, S., Ge, S., Chen, X., Ge, X., Chen, M., 2017. Hydrothermal carbonization of medical wastes and lignocellulosic biomass for solid fuel production from lab-scale to pilot-scale. *Energy* 118, 312–323.
<https://doi.org/10.1016/J.ENERGY.2016.12.047>
- Sun, Q., Khunsupat, R., Akato, K., Tao, J., Labbé, N., Gallego, N.C., Bozell, J.J., Rials, T.G., Tuskan, G.A., Tschaplinski, T.J., Naskar, A.K., Pu, Y., Ragauskas, A.J., 2016. A study of poplar organosolv lignin after melt rheology treatment as carbon fiber precursors. *Green Chem.* 18, 5015–5024.
<https://doi.org/10.1039/C6GC00977H>
- Toledano, A., Serrano, L., Labidi, J., 2011. Enhancement of Lignin Production from Olive Tree Pruning Integrated in a Green Biorefinery. *Ind. Eng. Chem. Res.* 50, 6573–6579. <https://doi.org/10.1021/ie102142f>
- Urruzola, I., Robles, E., Serrano, L., Labidi, J., 2014. Nanopaper from almond (*Prunus dulcis*) shell. *Cellulose* 21, 1619–1629. <https://doi.org/10.1007/s10570-014-0238-y>
- Vishtal, A.G., Kraslawski, A., 2011. Challenges in industrial applications of technical lignins. *BioResources* 6, 3547–3568. <https://doi.org/10.15376/biores.6.3.3547-3568>
- Wen, J.-L., Sun, S.-L., Xue, B.-L., Sun, R.-C., 2013. Recent Advances in Characterization of Lignin Polymer by Solution-State Nuclear Magnetic Resonance (NMR) Methodology. *Materials (Basel)*. 6, 359–391.
<https://doi.org/10.3390/ma6010359>
- Wild, P.J. de, Huijgen, W.J.J., Linden, R., Uil, H. den, Snelders, J., Benjelloun-Mlayah, B., 2015. Organosolv fractionation of lignocellulosic biomass for an integrated biorefinery. *NPT Procestechnol.* 1, 10–11.
- You, T.-T., Zhang, L.-M., Zhou, S.-K., Xu, F., 2015. Structural elucidation of lignin–carbohydrate complex (LCC) preparations and lignin from *Arundo donax* Linn. *Ind. Crops Prod.* 71, 65–74. <https://doi.org/10.1016/J.INDCROP.2015.03.070>
- Yuan, T.-Q., Sun, S.-N., Xu, F., Sun, R.-C., 2011. Characterization of Lignin Structures and Lignin–Carbohydrate Complex (LCC) Linkages by Quantitative ¹³C and 2D HSQC NMR Spectroscopy. *J. Agric. Food Chem.* 59, 10604–10614.

<https://doi.org/10.1021/jf2031549>

Zhang, W., Ma, Y., Wang, C., Li, S., Zhang, M., Chu, F., 2013. Preparation and properties of lignin–phenol–formaldehyde resins based on different biorefinery residues of agricultural biomass. *Ind. Crops Prod.* 43, 326–333.

<https://doi.org/10.1016/J.INDCROP.2012.07.037>

Zhao, X., Zhang, L., Liu, D., 2012. Biomass recalcitrance. Part I: the chemical compositions and physical structures affecting the enzymatic hydrolysis of lignocellulose. *Biofuels, Bioprod. Biorefining* 6, 465–482.

<https://doi.org/10.1002/bbb.1331>

Zheng, Y., Zhao, J., Xu, F., Li, Y., 2014. Pretreatment of lignocellulosic biomass for enhanced biogas production. *Prog. Energy Combust. Sci.* 42, 35–53.

<https://doi.org/10.1016/J.PECS.2014.01.001>

List of Tables:

Table 1. Initial composition of the raw material utilized in this work and the pulps remaining after each extraction step.

Sample	Cellulose (%)	Hemicelluloses (%)	Lignin (%)	Extractives (%)	Ashes (%)
AS	18.19±0.19	35.99±1.23	31.24±0.29	3.11±0.32	0.81±0.09
ASP1	42.97±0.61	29.21±0.33	15.97±0.78	4.42±0.41	ND ^(a) .
ASP2	48.06±0.75	23.83±0.41	15.02±0.63	1.68±0.21	ND ^(a)
ASP3	48.63±1.27	22.15±0.26	14.85±0.40	0.93±0.05	ND ^(a)

(a)– Non detectable

Table 2. Parameters for the evaluation of the efficiency of the different extraction cycles

Cycle	Overall yield ^a (% w/w)	Relative yield ^b (% w/w)	ASP yield ^c (% w/w)	Total amount of lignin extracted ^c (% w/w)
C1	16.75±0.29	79.95±1.16	39.21±0.79	79.95±1.16
C2	3.27±0.14	27.14±1.52	77.43±1.12	85.39±0.72
C3	0.96±0.09	15.86±2.75	85.05±2.19	87.73±0.34

(a)- Amount of lignin extracted related to mass of used biomass

(b)- Amount of lignin extracted related to the lignin content in the biomass used

(c)- Amount of pulp remaining after each extraction cycle

(d)- Percentage of lignin extracted after each related to the initial amount of lignin in biomass

Table 3. Mass balance of the whole process of organosolv delignification for the almond shells presented by steps

Sample	Cycle	Initial amount (g)	Amount dissolved (%)	Cellulose (g)	Hemicellulose (g)	Lignin (g)	Extractives (g)	Ashes (g)
AS		100		18.19	35.99	31.24	3.11	0.81
	C1		60.79					
ASP1		39.21		16.85	11.45	6.26	1.73	N.D ^a
	C2		22.57					
ASP2		30.36		14.59	7.23	4.56	0.51	N.D ^a
	C3		14.95					
ASP3		25.82		12.55	5.71	3.83	0.24	N.D ^a

Table 4. Parameters for the chemical characterization of liquors: pH, density, total dissolved solids (TDS), organic compounds (OC), inorganic compounds (IC) and lignin content in the liquor (LC)

Sample	pH	Density (g/cm ³)	TDS & OC (%)	IC (%)	LC (g/L)
Liquor C1	4.09±0.03	0.89±0.00	6.62±0.18	ND ^(a)	35.17±0.32
Liquor C2	4.29±0.01	0.86±0.00	2.20±0.10	ND ^(a)	8.34±0.38
Liquor C3	4.27±0.01	0.88±0.00	1.13±0.19	ND ^(a)	2.29±0.33

(a)– Non detectable

Table 5. Parameters measuring the chemical composition of lignin samples: klason lignin (KL), acid soluble lignin (ASL), total sugars (TS) and ashes.

Sample	KL (%)	ASL (%)	TS (%)	Glucose (%)	Xylose (%)	Ashes
L1	89.30±0.44	2.18±0.25	0.98±0.18	---	0.98±0.18	4.04±0.49
L2	92.07±0.89	2.05±0.80	1.62±0.07	---	1.62±0.07	3.59±1.31
L3	89.14±1.51	1.38±0.03	3.83±0.05	2.15±0.05	1.68±0.04	3.69±0.69

Table 6. Compounds identified and quantified in the different lignin samples

Molecule	m/z	Origin	Retention time (min)	L1	Content (%)	L2	L3
Styrene	104/103/78	B	5.894	0.02	---	---	---
Phenol	95/66/65	P	7.361	0.16	0.12	0.07	
4-methyl-Phenol	108/107/77	P	8.908	0.2	0.13	0.08	
Guaiacol	109/124/81	G	9.209	1.82	1.53	0.89	
4-Ethyl-phenol	107/122/77	P	10.556	0.2	---	---	---
4-Methyl-Guaiacol	138/123/95	G	11.23	2.28	1.74	1.39	
Catechol	110/64/81	C	11.397	0.13	---	---	---
3-methoxy catechol	140/125/97	C	13.124	0.47	0.35	0.25	
4-ethyl guaiacol	137/152/122	G	13.615	1.02	0.55	0.47	
4-vinylguaiacol	150/135/107/77	G	14.834	3.21	4.06	2.5	
p-allyl phenol	134/133/107	P	15.55	0.07	0.06	0.02	
Syringol	154/139/111/96	S	15.908	3.6	2.85	1.62	
Eugenol	164/149/131/77	G	16.035	0.79	0.74	0.46	
4-Propylguaiacol	137/166/122	G	16.266	0.31	0.16	0.12	
Vanillin	151/152/81	G	17.086	1.71	2.02	1.23	
cis-isoeugenol	164/149/77/131	G	17.225	0.48	0.41	0.23	
4-methyl syringol	168/153/125	S	18.114	8.01	3.32	2.58	
trans-eugenol	164/149/77/103	G	18.097	---	3.52	1.4	
4-Propylguaiacol	137/166/122	G	18.299	0.19	0.84	0.61	
acetoguaiacone	151/166/123	G	18.825	0.82	1.34	0.77	
4-ethyl syringol	167/182/168/77	S	19.489	1.71	1.05	0.81	
Guaiacyl acetone	137/180/122	G	19.604	0.92	0.46	0.889	
4-vinylsyringol	180/137/165	S	20.147	4.2	5.1	2.93	
Propioguaiacone	151/180/123	G	20.413	0.53	0.48	---	---
4-allylsyringol	194/91/119	S	20.696	1.66	1.4	0.68	
4-Propylsyringol	167/196//168/123	S	20.777	0.67	---	---	---
cis-4-allylsyringol	194/91/179	S	21.377	1.59	1.4	0.85	
syringaldehyde	182/181/167/111	S	21.568	3.08	3.02	1.79	
Propenylsyringol	192/177/131	S	21.741	---	0.77	0.31	
trans-4-allylsyringol	194/91/179	S	22.082	8	8.75	4.12	
Acetosyringone	181/196/153	S	22.498	3.22	3.11	1.85	
Syringylacetone	167/210/168	S	22.931	2.07	2.64	1.74	
Propiosyringone	181/210/182	S	23.543	1.66	1.37	---	---
Synaphthaldehyde	208/165/137/180	S	25.212	---	---	2.71	
Synapaldehyde	208/165/137/180	S	25.535	2.4	---	---	---
Total benzene derivatives					0.02	---	---
Total phenol derivatives					0.63	0.31	0.17
Total catechol derivatives					0.6	0.35	0.25

Total guaiacyl derivatives	14.08	17.85	10.95
Total syringyl derivatives	41.87	34.78	21.99
Ratio S/G	2.97	1.95	2.01

Table 7. Relative abundance of main inter-unit linkages expressed as percentage of side chains involved

Type of linkage	Relative abundance in lignin samples (%)		
	L1	L2	L3
β -O-4' aryl ether (A, A')	22.41	22.68	24.67
β - β resinols (B)	1.37	1.23	1.15
β -5' phenylcoumarane (C)	5.09	4.07	5.50
-OCH ₃ methoxyl groups	70.32	69.6	66.3
Lignin carbohydrate complex (LCC)			
Benzyl ether LCC	0.81	1.87	2.37
Ratio S/G	1.38	1.28	1.14

Table 8. Thermogravimetric parameters of the different lignin samples

Sample	T _{5%} (°C)	T _{max} (°C)	Residue at 800°C (wt.%)
L1	258.64	370.60	38.73
L2	252.50	369.52	42.35
L3	228.91	363.48	42.68

List of figures

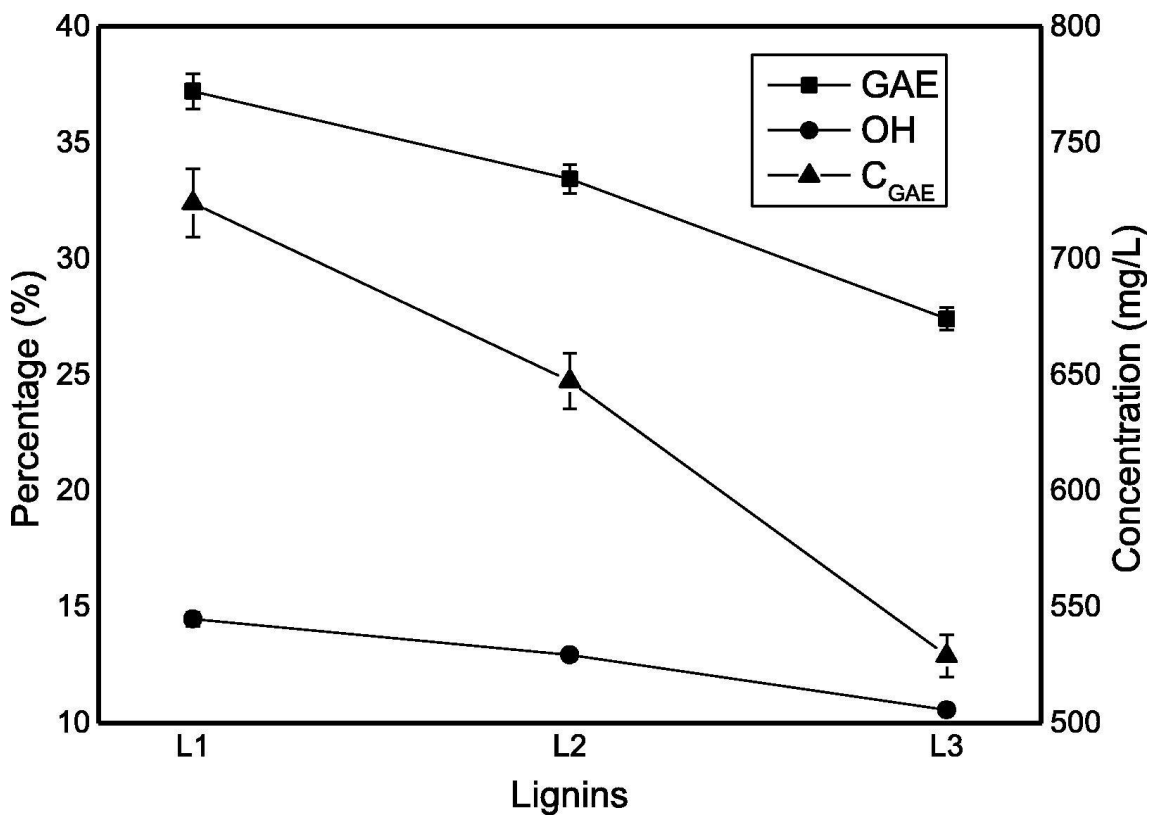


Figure 1. Variation of the different parameters calculated for the phenolic content of the lignin samples.

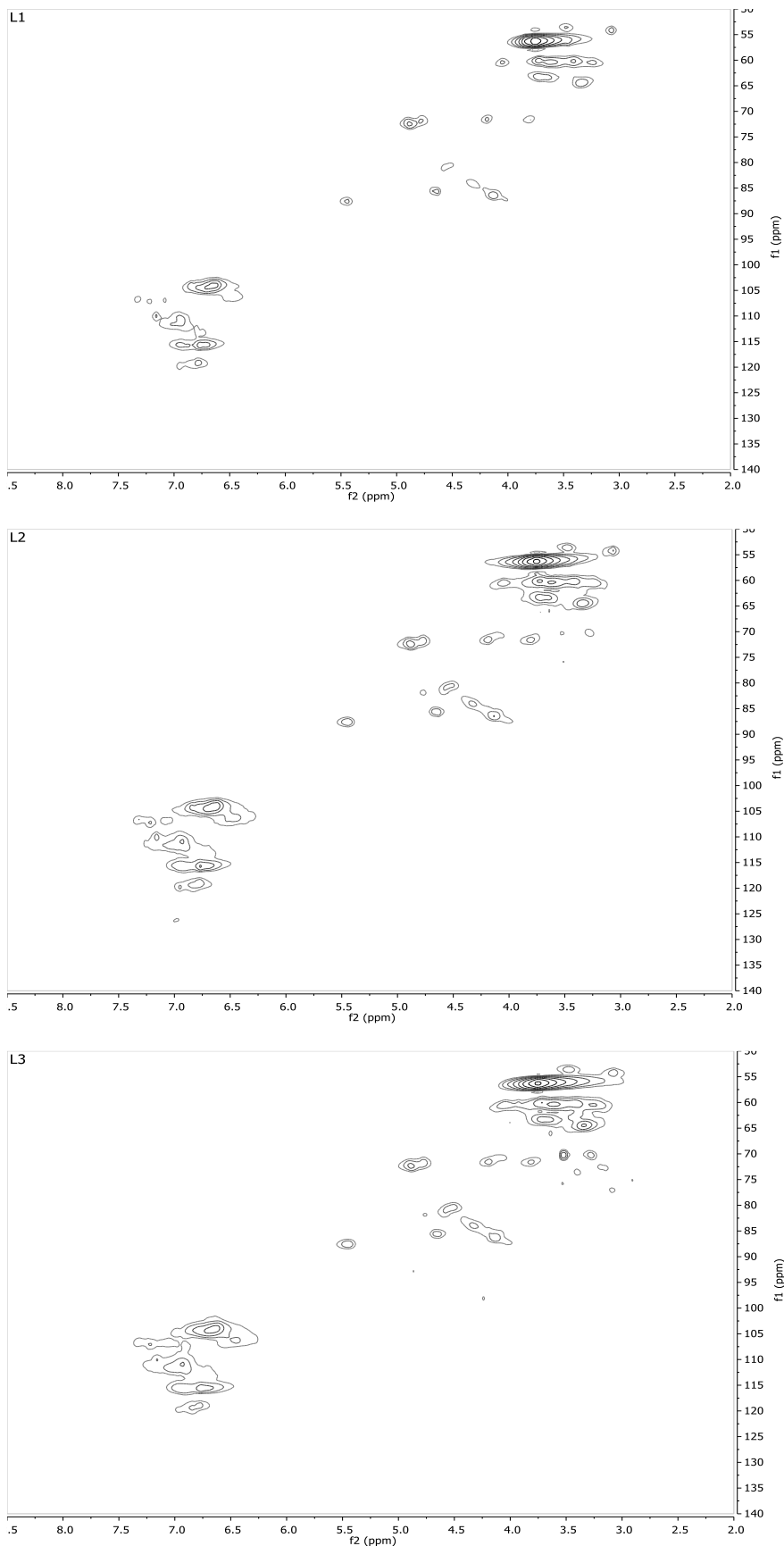


Figure 2. 2D-HQSC-NMR spectra of the different lignin samples

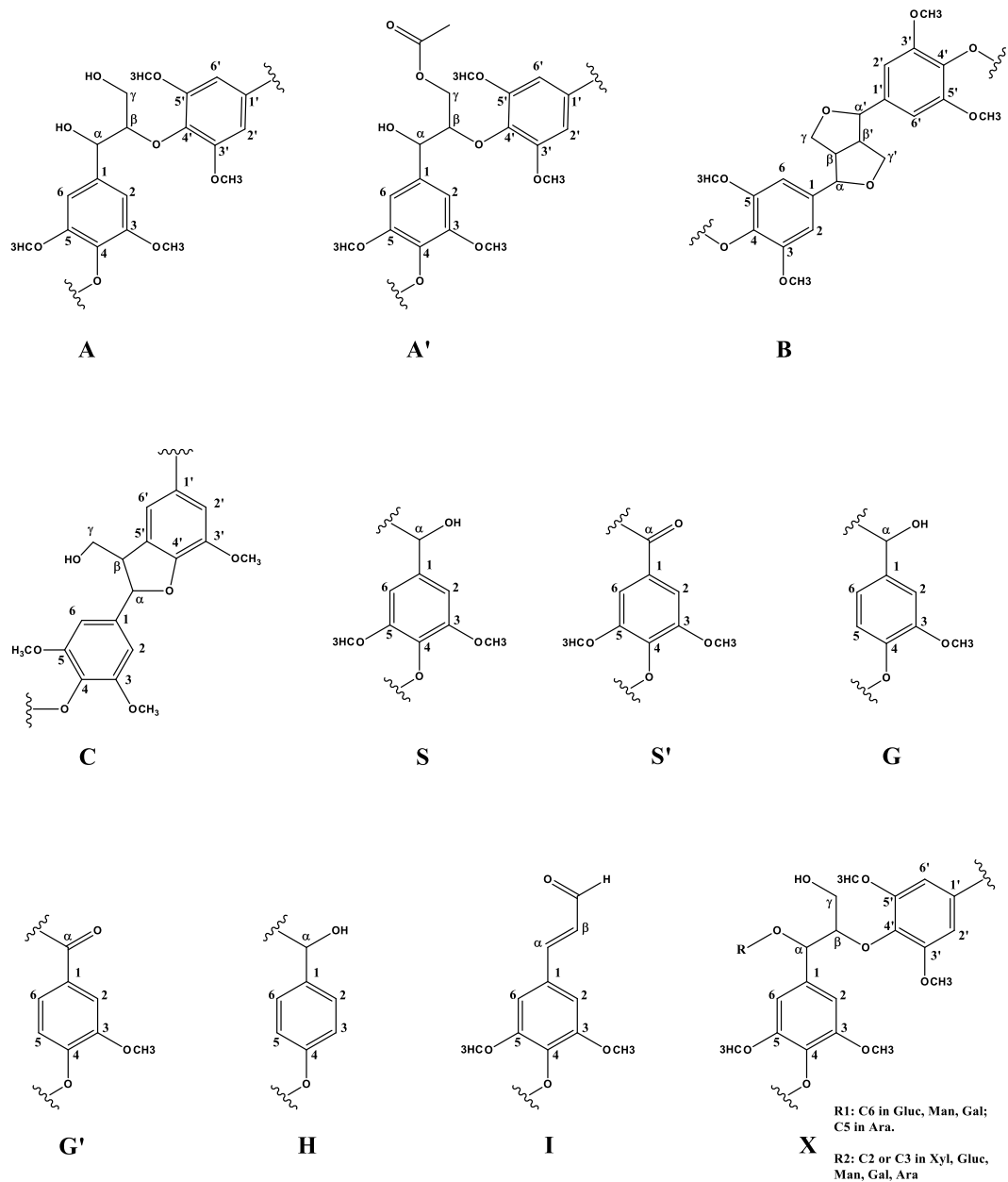


Figure 3. Main structures involving the different side chains and aromatics units detected by 2D-HQSC-NMR of lignin samples L1, L2 and L3: (A) β -O-4' aryl ether linkages with a free hydroxyl group at the γ -carbon; (A') β -O-4' aryl ether linkages with acetylated hydroxyl group at the γ -carbon; (B) resinol substructures composed of β - β , α -O- γ' and γ -O- α' linkages; (C) phenyl coumarane substructures composed of β -5' and α -O-4' linkages; (S) syringyl units; (S') oxidized syringyl units with a carboxyl group at C_α ; (G) guaiacyl units, (G') oxidized guaiacyl units

with a carboxyl group at C_α; (I) cinnamaldehyde end groups and (X) Benzylether lignin carbohydrate complexes (LCC) with C1-linkages between the α-position of lignin and the primary hydroxyl group of carbohydrate.

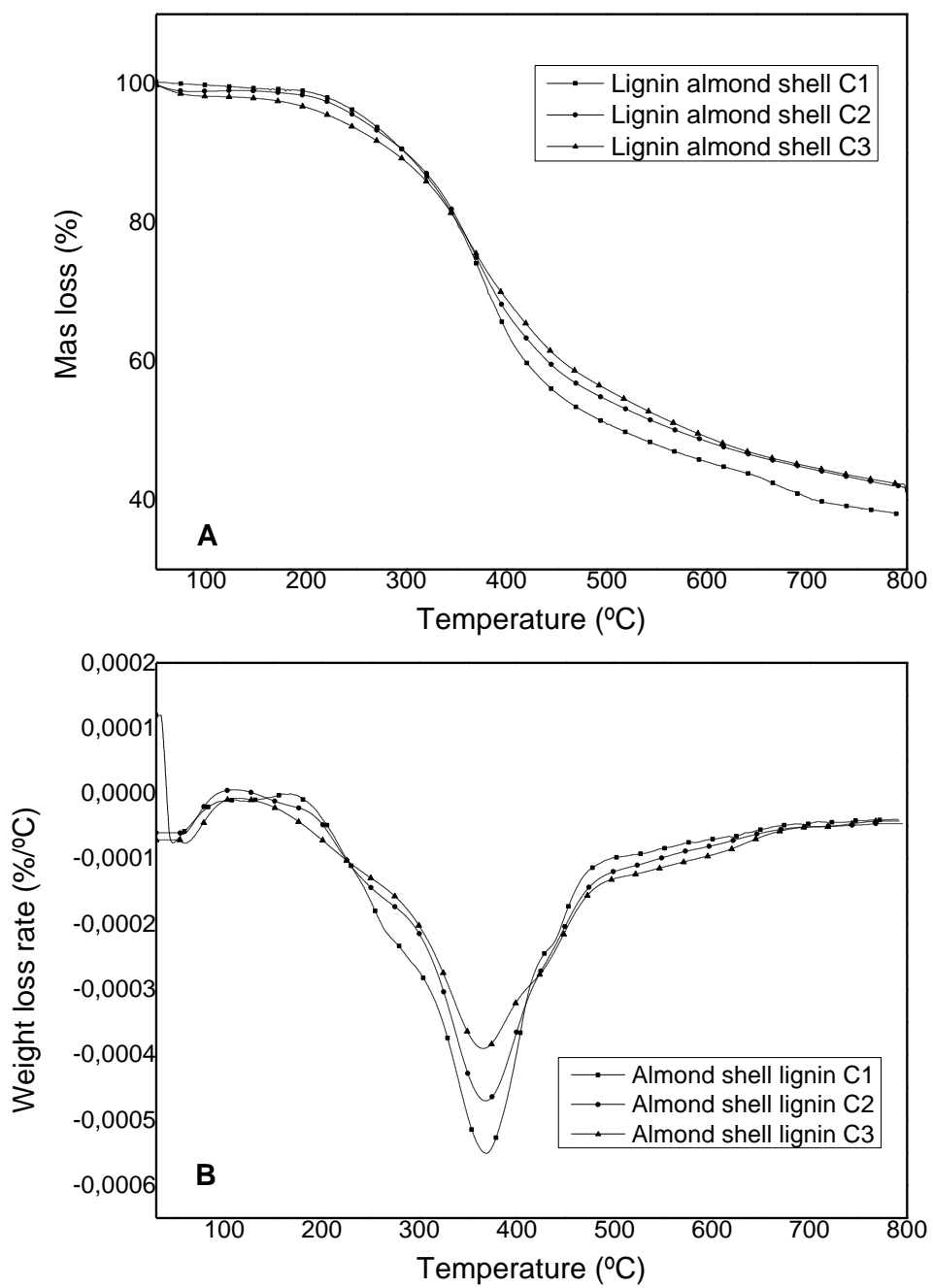


Figure 4. Thermogravimetric (A) and derivative thermogravimetric (B) curves for the lignins extracted from the different cycles

SUPPLEMENTARY INFORMATION:

1. Process set up description

In figure SI-1 the scheme of the multistage delignification process is shown. This process was composed of three sequential organosolv pulping cycles. The diagram displayed in figure S1 shows the different streams derived from the process. In the first cycle (C1), the almond shells (AS) underwent organosolv pulping process yielding two different streams i.e. black liquor (BL1) and almond shells pulp (ASP1) from the first cycle. The former was used for the precipitation of the lignin from the first cycle (L1) whereas the almond shells pulp (ASP1) was employed as raw material for the second cycle (C2). In this second cycle, the almond shells pulp (ASP1) went through another organosolv pulping process. Again two separate products were obtained namely black liquor (BL2) and almond shells pulp (ASP2) from the second cycle. The lignin from the second cycle (L2) was anew precipitated the lignin from the black liquor (BL2) and the almond shells pulp (ASP2) was utilized as the starting material from the third cycle (C3). This last cycle was implemented analogously to the previous ones resulting in black liquor (BL3) and precipitated lignin (L3) from the third cycle and almond shells pulp (ASP3).

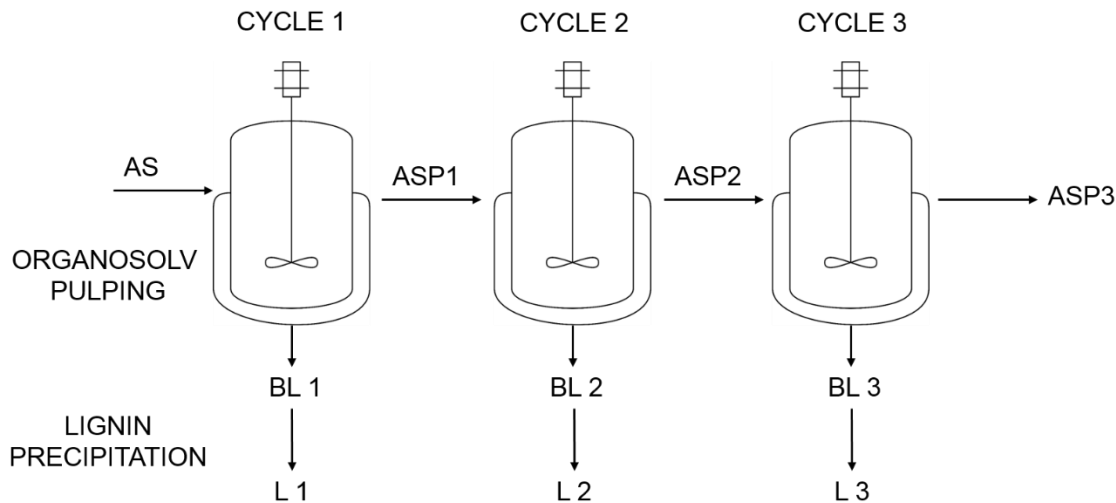


Figure SI1. Diagram showing the process set up for the organosolv extraction of lignin from almond shells and almond shells pulps: (AS) almond shells; (BL1) black liquor from first cycle; (L1) lignin extracted from first cycle; (ASP1) almond shells pulp from first cycle; (BL2) black liquor from second cycle; (L2) lignin extracted from second cycle; (ASP2) almond shells pulp from second cycle; (BL3) black liquor from third cycle; (L3) lignin extracted from third cycle; (ASP3) almond shells pulp from third cycle

2. Chemical characterization of lignins

Here the procedure employed for the chemical characterization of the lignins samples is comprehensively described. This procedure was carried out in two steps. First 3.75 mL of H₂SO₄ (72%) were added to 0.375 g lignin samples and then the mixture was set at 30°C for 1h. After this period, the samples were diluted with 36.25 mL deionized water and heated up to 100°C during 3h. Following to that, the mixture was cooled down before filtering it using a G4 glass filter crucible. From the solid remaining, the Klason lignin (KL) content was calculated. On the other side, from the liquid phase the Acid soluble lignin (ASL) was determined via spectrophotometry using a Jasco V-630 UV equipment with UV

quartz cells and a 10mm light path. For this purpose, the filtrate samples were diluted with H₂SO₄ 1M and the absorbance values were obtained at 205 nm. Only absorbance values in the range between 0.1-0.8 were considered (TAPPI UM250 um-83). The Acid soluble lignin content was calculated using equation 2 where A refers to the absorbance values measured at 205 nm, D is the dilution factor, V is the filtrate volume obtained, ε the extinction coefficient (110 L·cm·g⁻¹) and m is the sample weight before the hydrolysis.

$$\text{Acid soluble lignin (\%)} = (A \cdot D \cdot V) / (\varepsilon \cdot m) \quad (\text{eq.1})$$

The sugar content of the lignin samples (impurities) was obtained from the filtrates. For the determination of the main monosaccharides (glucose, xylose and arabinose) High Performance Liquid Chromatography (HPLC) was employed, with a Jasco LC Net II/ADC chromatograph equipped with a refractive index detector and a diode array detector. A sample of the liquid phase was used to quantify the main monosaccharides and degradation products employing a Phenomenex Rezex ROA column; the mobile phase (0.005N H₂SO₄) was eluted at a flow rate of 0.35 mL/min at 40 °C. Standards of high purity of D-(+)-glucose, D-(+)-xylose and D-(-)-arabinose were employed as calibration.

3. Temperature selection for pyrolysis analysis

In table SI-1 the relative content of the different compounds produced in the pyrolysis of L1 at several temperatures was shown.

Table SI-1. Variation of the phenolic compounds content and their subgroups at different pyrolytic temperatures for L1

Unit type	Relative content (%)		
	T = 500 °C	T = 600 °C	T = 700 °C

Syringol	33.30	41.87	23.99
Guaiacol	15.9	14.08	18.00
Catechol	0.75	0.6	7.89
Phenol	0.42	0.63	2.66
Benzene	0.02	0.02	0.39
Total phenolics	50.37	57.18	53.21

In the previous data it can be observed how there was a slight increase in the selectivity at 600 °C (from 50,37% to 57,18%) and again another small reduction at 700°C (from 57,18% to 53,21%). Thus it was concluded that the highest selectivity of phenolic compounds was reached at 600°C. This was in accordance with the results of Wang et al 2015 (Wang et al., 2015) and therefore this temperature was selected for carrying out the pyrolysis analysis of the rest of the lignin samples.

Regarding the different phenolic compounds, the most abundant group was the syringol type. Indeed, its relative content is considerably higher than the rest of the other phenolic subgroups. On the contrary, the benzene type was the one with the tiniest contribution to the phenols and was neglected. The phenol and catechol types groups did not show a substantial change in the relative contents between 500-600 °C. However as the temperature increased to 700 °C they reached their maximum values. Guaiacol type compounds went through a slight decrease first to reach their maximum content at 700 °C.

From the previous results, it could be concluded that the increase in the temperature did not have a crucial influence on the total content of phenolic compounds identified, but it did on the different subgroups. Furthermore, the increment of the pyrolytic temperature has a direct impact mainly over the syringol type group, whose relative content decreased dramatically. This reduction was due to the fact that at high temperatures, demethoxylation reactions happened

degrading syringol type subunits into other types (Liu et al., 2016). Thus, the demethoxylation reactions could be responsible for the increase of the phenol, catechol and guaiacol types groups relative content at the highest temperature. Consequently, they might be benefited by the demethoxylated syringol type units as reported by Ma 2016 (Ma et al., 2016).

References:

- Liu, C., Hu, J., Zhang, H., Xiao, R., 2016. Thermal conversion of lignin to phenols: Relevance between chemical structure and pyrolysis behaviors. Fuel 182, 864–870. <https://doi.org/10.1016/J.FUEL.2016.05.104>
- Ma, Z., Sun, Q., Ye, J., Yao, Q., Zhao, C., 2016. Study on the thermal degradation behaviors and kinetics of alkali lignin for production of phenolic-rich bio-oil using TGA–FTIR and Py–GC/MS. J. Anal. Appl. Pyrolysis 117, 116–124. <https://doi.org/10.1016/J.JAAP.2015.12.007>
- Wang, S., Ru, B., Lin, H., Sun, W., Luo, Z., 2015. Pyrolysis behaviors of four lignin polymers isolated from the same pine wood. Bioresour. Technol. 182, 120–127. <https://doi.org/10.1016/J.BIORTECH.2015.01.127>